machines

MDPI

Article

4D Printing: A Methodical Approach to Product Development Using Smart Materials

Stefan Junk [1], Henning Einloth [1,*] and Dirk Velten [2]

[1] Laboratory of Rapid Prototyping, Department of Business and Industrial Engineering, Offenburg University of Applied Sciences, Klosterstr. 14, 77723 Gengenbach, Germany; stefan.junk@hs-offenburg.de
[2] Department of Mechanical and Process Engineering, Offenburg University of Applied Sciences, Badstr. 24, 77652 Offenburg, Germany; dirk.velten@hs-offenburg.de
* Correspondence: henning.einloth@hs-offenburg.de

Abstract: In 4D printing, an additively manufactured component is given the ability to change its shape or function in an intended and useful manner over time. The technology of 4D printing is still in an early stage of development. Nevertheless, interesting research and initial applications exist in the literature. In this work, a novel methodical approach is presented that helps transfer existing 4D printing research results and knowledge into solving application tasks systematically. Moreover, two different smart materials are analyzed, used, and combined following the presented methodical approach to solving the given task in the form of recovering an object from a poorly accessible space. This is implemented by self-positioning, grabbing, and extracting the target object. The first smart material used to realize these tasks is a shape-memory polymer, while the second is a polymer-based magnetic composite. In addition to the presentation and detailed implementation of the methodical approach, the potentials and behavior of the two smart materials are further examined and narrowed down as a result of the investigation. The results show that the developed methodical approach contributes to moving 4D printing closer toward a viable alternative to existing technologies due to its problem-oriented nature.

Keywords: 4D printing; smart materials; shape-memory polymers; polymer-based magnetic composites; methodical approach

Citation: Junk, S.; Einloth, H.; Velten, D. 4D Printing: A Methodical Approach to Product Development Using Smart Materials. *Machines* **2023**, *11*, 1035. https://doi.org/10.3390/machines11111035

Academic Editors: Zbigniew Pilch and César Vasques

Received: 28 September 2023
Revised: 11 October 2023
Accepted: 4 November 2023
Published: 20 November 2023

1. Introduction

The technology of additive manufacturing (AM) has developed rapidly in recent years. In the course of the development of 3D printing, various AM processes exist, and numerous different materials can be processed. With the help of 4D printing, the previously static, 3D-printed components are given the ability to react dynamically to changing stimuli from the environment with a desired change in shape or function [1]. In order to implement this, materials are required that allow the shape or function to be changed selectively by an external stimulus. These materials are also referred to as smart materials [2–5].

In addition to the use of smart materials, there are other important core elements in 4D printing. These include the stimulus used to trigger the change in shape or function, the additive manufacturing process, and the modeling and construction of the part. For some smart materials, such as shape-memory polymers, the programming of the smart material is another important core element [6–8].

Currently, the technology of 4D printing is at an early stage of development. Much research is needed to further develop the technology and establish it in applications [6,9]. Future promising and interesting areas of application may include medical fields or the field of soft robotics [8,10,11].

PLA and composite materials are common materials in 4D printing and have been thoroughly investigated [12,13]. For example, grippers were developed that consist of a shape-memory polymer (SMP). These are able to use the shape-memory effect (SME) of the

smart material to selectively grasp an object [14]. Based on the same principle, researchers developed a prototype stent fabricated from a magnetic composite material. The fine iron particles contained in the SMP matrix of the composite material allow the stent to be heated remotely via an alternating magnetic field, triggering the SME of the SMP matrix. In this way, the stent unfolds and performs the desired function of dilating a narrowed vessel [15].

By manipulating the printing parameters consciously and purposefully in bi-layered structures consisting of SMPs, researchers are able to skip the classic programming step by causing pre-strain during the printing process. With this technique, soft robots or hinges can be made ready for use directly from the print bed by applying heat [16–19].

In addition to SMPs, hydrogels are commonly used smart materials in 4D printing [20]. Hydrogels can absorb and store large amounts of water, which allows them to change their volume to a large extent [11]. In initial work on 4D printing, hydrogels are used in conjunction with rigid polymers to trigger mechanics through the change in volume upon contact with water, causing a change in shape [1,21]. Following the same approach, researchers present a technique where the hydration of hydrogels in tri-layered structures is used to perform movements from 2D to 3D structures through integrated local bi-layer hinges. The authors used this technique to realize complex origami shapes [22].

By using a smart hydrogel whose volume changes as a function of temperature, researchers are producing a smart valve. This is capable of controlling the flow of water through the valve's flow channel as a function of temperature. The valve is able to reduce the water flow by up to 99% when the critical temperature is exceeded. This process can be performed reversibly [23]. Similar to this, researchers used thermal-responsive hydrogels to manage a controlled drug release according to ambient temperature. The drug release behavior can be controlled by varying the shell thickness of the capsules, and it highly depends on the ambient temperature. The results show promising applications in smart drug release [24].

Recently, smart hydrogels have been used to show shape-memory and self-healing abilities. These abilities occur near the human body temperature, showing promising applications in the field of biomedicine. To demonstrate shape memory and self-healing, different specimens were made and examined, including a robotic hand to demonstrate shape memory and a manually cut specimen to investigate self-healing [25].

In other work, researchers are combining the SME with hydrogel volume change to perform targeted grasp-and-release movements of an object [26].

By using a humidity-sensitive smart hydrogel, an artificial, biomimetic, seed-inspired soft robot is presented, which is capable of exploring and adapting to a sample soil while also being able to lift up to 100 times its own body weight when exposed to changes in humidity. It is made of a hygroscopic inactive polycaprolactone substrate printed with a material extrusion (MEX) printer in combination with electrospinning hygroscopic fibers on its surface [27].

Another interesting material commonly used in 4D printing is liquid crystal elastomers (LCEs). Researchers used the direct ink writing process to align the mesogen domains of the LCE along the printing direction. When heated above their nematic–isotropic temperature, the LCE contracts parallel to the direction of the nematic director, which is parallel to the direction of the mesogen alignment previously set by the printing path. Using this technique, the authors create artificial muscles and perform complex 2D and 3D shape changes capable of reversibly changing their shape with potential applications in soft robotics [28].

In addition to SMPs, bi-layered structures, hydrogels, and LCEs, magnetic composite materials are being used in 4D printing. These materials impress with a fast response time and much better reversibility compared to SMPs and hydrogels. In the literature, researchers use an elastic matrix material in which fine, hard magnetic particles are embedded. By manipulating the orientation or magnetization of these particles accordingly, it is possible to create magnetic domains with different polarizations within a component. This allows for complex movement of the component, caused and controlled by an external

magnetic field. In this case, the elastic matrix of the composite material acts as a resetting mechanism once the external magnetic field is switched off. These properties ensure reversibility, repeatability, and controllability of the change in shape or function [29,30].

In this work, a new methodical approach for the development of 4D printed components is presented and followed in order to systematically solve a given task in the form of an application example. This new approach is based on classical design methodology in order to solve technical problems in a methodical, comprehensible, and application-oriented way. Furthermore, the approach is intended to support the transfer of existing knowledge in the field of 4D printing to technical applications. As the focus of existing work in the literature tends to be on a particular material and a material-related, non-flexible application, this approach aims to adopt a holistic and problem-solving approach. For 4D printing to become a viable alternative to existing technologies, it is essential to start from a problem-oriented point of view. As a special feature, two smart materials are combined within the scope of the presented application example in order to solve the given task. Both smart materials used will be investigated to identify and narrow down their potential. Important findings and future starting points for further research work are derived from the results.

2. Materials and Methods

2.1. Methods

First, the developed methodical approach for the development of 4D printed components is presented [31]. This is based on classical design methodology in order to follow a systematic and application-oriented approach during the development of the components [32,33]. Overall, it is composed of four main steps, which are:

- Task clarification;
- Conceptual design;
- Embodiment design;
- Manufacturing.

In the first main step, "Task clarification", a basic and comprehensive understanding of the task is created. This highlights the main problem to be solved. It is also necessary to define the most important requirements. One of the most important points in this phase is the recognition of the overall function of the component. Here, it is useful to divide the overall function into less complex sub-functions. This simplifies the subsequent search for a solution. By fulfilling all sub-functions, the overall function of the component is ultimately also fulfilled.

As soon as the overall and sub-functions are known, the search for solution principles for the individual sub-functions begins with the second main step, "Conceptual design". Their implementation refers to the knowledge gained to date in the field of 4D printing. The focus is on how and with which smart materials and stimuli the sub-functions can be fulfilled. For example, one solution principle is developed using an SMP, whereas another solution principle refers to the use of a hydrogel. The use of a magnetic composite or other smart materials to fulfill the respective sub-function can also be included in the solution found here. In principle, all published findings in the field of 4D printing can be integrated. It is important to note that the sub-functions are ultimately linked back together in such a way that the overall function of the component is fulfilled. For this purpose, the use of a morphological box is recommended in order to identify suitable solution combinations. A structured evaluation procedure, such as a utility analysis, can be helpful for selecting the most suitable solution combination.

After the selection, the individual solution principles for the sub-functions are specified and elaborated in the third main step, "Embodiment design". Starting from the optimal solution principle for each sub-function, a first design is prepared, based on a theoretical model of the task. Subsequently, the first design is iteratively analyzed, dimensioned, and optimized by producing and using prototypes until a satisfactory result with reliable

fulfillment of the sub-function is achieved. The result of this main step is the final design and its corresponding CAD models.

In the last main step, "Manufacturing", the developed components are manufactured on a suitable 3D printer. The additive manufacturing process to be used depends on the selected smart material, as only certain additive manufacturing processes can be considered. In some cases, such as in the case of an SMP, the 3D-printed components still have to be brought to an operational state. The assembly of the subsystems into a complete system is also carried out in this step. Once all the main steps have been completed, the 4D printed component is able to successfully fulfill the overall function of solving the given task or problem.

2.2. Application Example

In order to carry out the developed procedure practically, it is applied in connection with an application example. The given task is the recovery of a target object from a poorly accessible space. For the physical representation of this poorly accessible space, a bottle is used. To enable targeted extraction, the target to be recovered is located in the center of the bottle base. A schematic illustration of the task is shown in Figure 1.

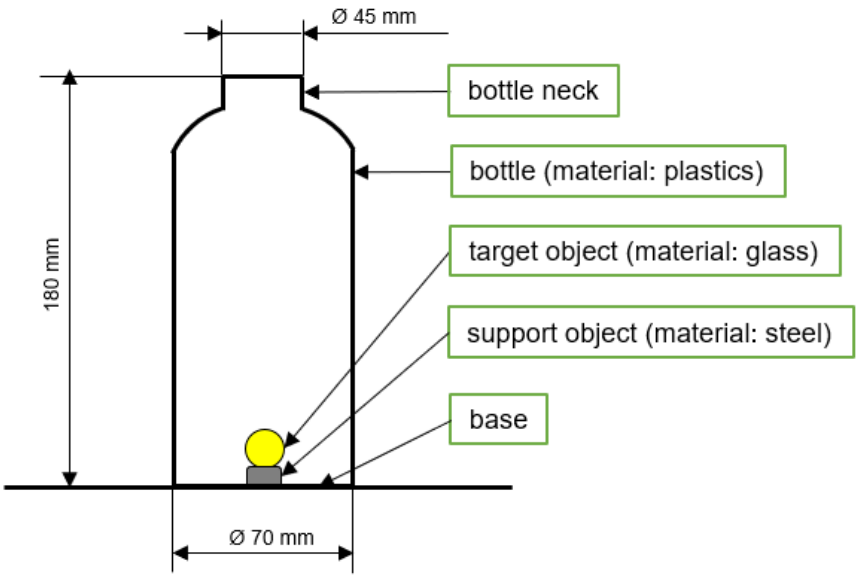

Figure 1. Schematic illustration of the given problem represented by a bottle with a bottleneck, the target object, and the associated dimensions for the physical representation of the poorly accessible space based on [31].

2.3. Materials

Two different smart materials are used to realize the solution principles, which are presented in detail in Section 3. The first smart material is an SMP consisting of polylactide (PLA). PLA is a thermoplastic material in the form of a filament, which can be processed on a MEX 3D printer. The exact name of the material is "Prusament PLA", which is manufactured by Prusa Polymers in the Czech Republic. Table 1 shows an overview of the most important properties of the material.

Table 1. Properties of the material "Prusament PLA".

Property	Unit	Value
Density	g/cm^3	1.24
Glass Transition Temperature	°C	55
Tensile Yield Strength (Filament)	MPa	57

The second smart material used is a magnetic composite material. It consists of PLA, which forms the carrier matrix of the composite material. In addition, fine iron particles are added to the composite material to achieve magnetic properties. Since the carrier matrix is made of PLA, this composite material can also be processed on a MEX 3D printer. The exact name of the composite material used is "Iron-filled Metal Composite PLA", which is manufactured by Protopasta in Vancouver, Washington, USA. Table 2 presents an overview of the most important properties of the material.

Table 2. Properties of the composite material "Iron-filled Metal Composite PLA".

Property	Unit	Value
Density	g/cm^3	1.85
Glass Transition Temperature	°C	60
Tensile Yield Strength (Filament)	MPa	N/A

The "Original Prusa i3 MK3S+" 3D printer, manufactured by Prusa Research a.s. in the Czech Republic, is used to process these two smart materials.

3. Results

3.1. Task Clarification

In the first step, the most important requirements for the component are defined. In this example, this is compliance with the maximum permitted width of less than 45 mm so that the component can pass through the neck of the bottle into the interior during subsequent use.

The identification of the overall function is the next step. This, according to the problem, is the one-time recovery of the target object from inside the bottle. The overall function can be divided into three sub-functions. These include the correct positioning of the entire component, gripping the target object, and extracting the target object from the poorly accessible space. In the end, the appropriate combination of all three sub-functions in their entirety contributes to the fulfillment of the overall function. Figure 2 shows the division of the overall function into the three sub-functions.

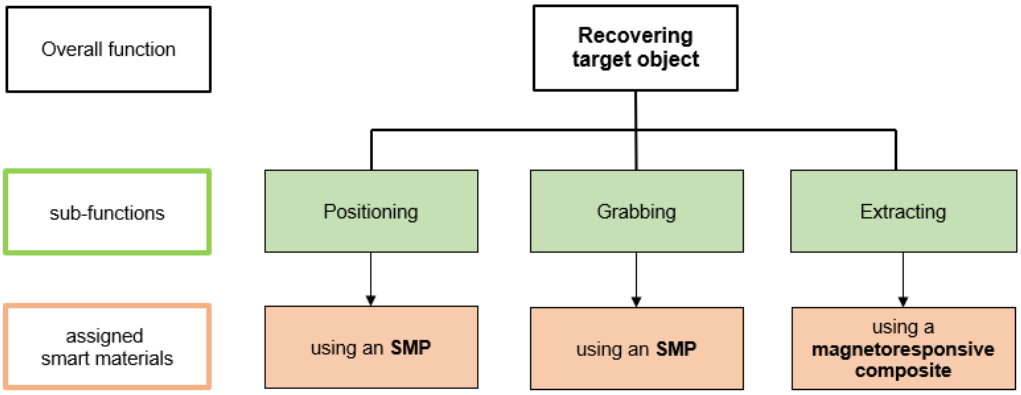

Figure 2. Division of the overall function of the component into the sub-functions and their assigned smart materials to fulfill the sub-functions based on [31].

3.2. Conceptual Design

According to the methodological approach, as many different solution principles and implementation concepts for the sub-functions as possible should be worked out in this step. These are then used to form appropriate solution combinations using the morphological box, and utility analysis is used to identify the optimal solution combination to fulfill the overall function. At this point, this step is deliberately omitted so that the two smart materials in the form of an SMP and a magnetic composite material can be included in the

solution finding because of their simple, more accessible printability. The focus of this work is, therefore, on the use of these two smart materials to solve the given task.

Before a decision is made as to which subsystems are made of which smart materials to solve the sub-functions, the properties of the two smart materials are examined in detail, and their potentials are narrowed down.

3.2.1. Shape-Memory Polymers

When using SMPs, the SME is used to cause a change in shape or function. The SMP is able to remember its original shape after temporary deformation. The temporary shape is taught to the SMP by heating it above its glass transition temperature T_G and then deforming it. The external stress is maintained until the temperature of the SMP has dropped back below T_G. In this way, the SMP maintains its temporary shape. This process is also called the programming phase. When the SMP is heated above T_G again, the shape recovery phase begins and the SMP recovers its original shape [10]. This allows the SMP to switch between two shapes but requires the SMP to be reprogrammed after each shape recovery. The shape recovery capability decreases significantly as the number of cycles increases. PLA is an excellent SMP suitable and readily available for FDM 3D printing, which is also used in this work.

3.2.2. Magnetic Composite Material

The magnetic composite material used in this work consists of a PLA carrier matrix mixed with fine iron particles. Iron is a soft magnetic material. It has low remanence and low coercivity, unlike hard magnetic materials, such as a neodymium–iron–boron alloy (NdFeB). Coercivity is the magnetic field strength required to completely demagnetize the material. The remanence is the remaining magnetic flux density in the material when the external magnetic field is removed. Due to the low remanence of iron, the magnetization of the iron particles cannot be maintained after the external magnetic field is removed. Also, the low coercivity means that iron can be demagnetized very easily. As a result, domains with partially different polarizations cannot be created with this material, which is the prerequisite for more complex, magnetic field-controlled movements of the component. Due to the low coercivity and remanence of the iron particles, only magnetic attraction can be used.

The carrier matrix of the composite material consists of PLA, which is rigid at room temperature and cannot be deformed. Above a temperature of approx. 60 °C, the T_G is exceeded and deformability is given.

Based on these findings, the positioning and gripping systems are implemented by using an SMP, while the extraction system is implemented by using the magnetic composite material. This decision is based on the fact that positioning and gripping involve complex, multidimensional movements that significantly exceed the potential of the magnetic composite material used in this example. For extraction, the use of the magnetic composite material is perfectly suitable due to the less complex movement. Figure 2 sums up the sub-functions and their assigned smart materials.

3.3. Embodiment Design

For the three sub-functions, the first designs are now made based on a theoretical model of the task. These are explained in the following sections. All CAD models are designed with CATIA V5.

3.3.1. First Designs

Positioning system:

The positioning system is implemented in the form of a six-arm system. Three arms are located on the underside of the main body of the positioning system and the other three arms are on the upper side. These are arranged at an angle of 120°, respectively. To

increase the accuracy of the alignment, the arms on the bottom and top sides are offset from each other.

The idea behind this design is to fold the arms up or down during the programming of the SMP, where their tips meet on the extended axis of the center hole. This temporarily brings the width of the positioning system for placement inside the bottle below the permitted width of 45 mm. If the external stimulus is now applied by heating the positioning system above T_G, the SME engages, and the arms strive to their original horizontal shape. Since this movement is restricted by the bottle walls, the arms of the positioning system press against the bottle walls and the component positions itself above the center of the bottle base at a certain height. The pockets on the top and bottom of the component are used for later integration of the gripping and extraction system. The first design of the positioning system in the form of a CAD model can be seen in Figure 3.

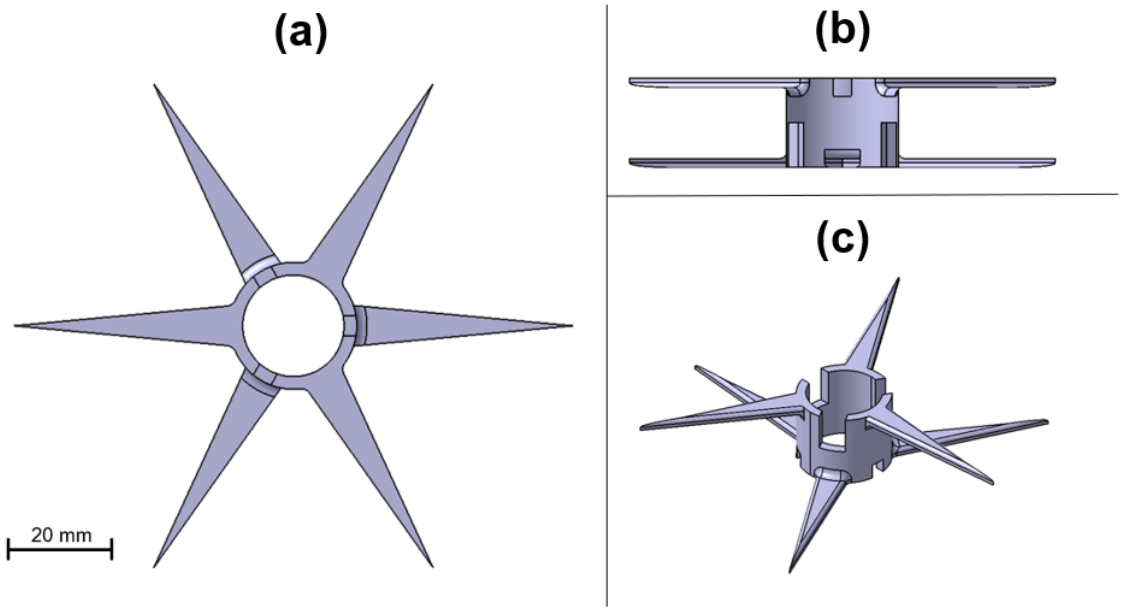

Figure 3. First design of the positioning system in different views: (**a**) top view, (**b**) side view, (**c**) three-dimensional view.

Gripping system:

A three-arm system is used for the gripping system in order to keep the effort required for programming the SMP as low as possible. In addition, three arms are sufficient for gripping the target object safely. Similar to the positioning system, the gripper arms are also arranged at an angle of 120° to each other.

The SME is also used in this design. The gripper arms are first opened wide by folding them backward by almost 180°. To realize this, a pocket is inserted below each gripper arm. This also ensures that the gripper system does not exceed the permitted width of 45 mm. After the SME is triggered by heating the gripping system via T_G, the original, the initially closed shape of the gripping arms is restored. The target object is gripped firmly during this operation. With the help of three small extensions at the end of the middle cylinder, the gripping system is attached to the positioning system. A groove is placed on the bottom of the gripping system for later integration of the extraction system. Figure 4 shows the first design of the gripping system in various views.

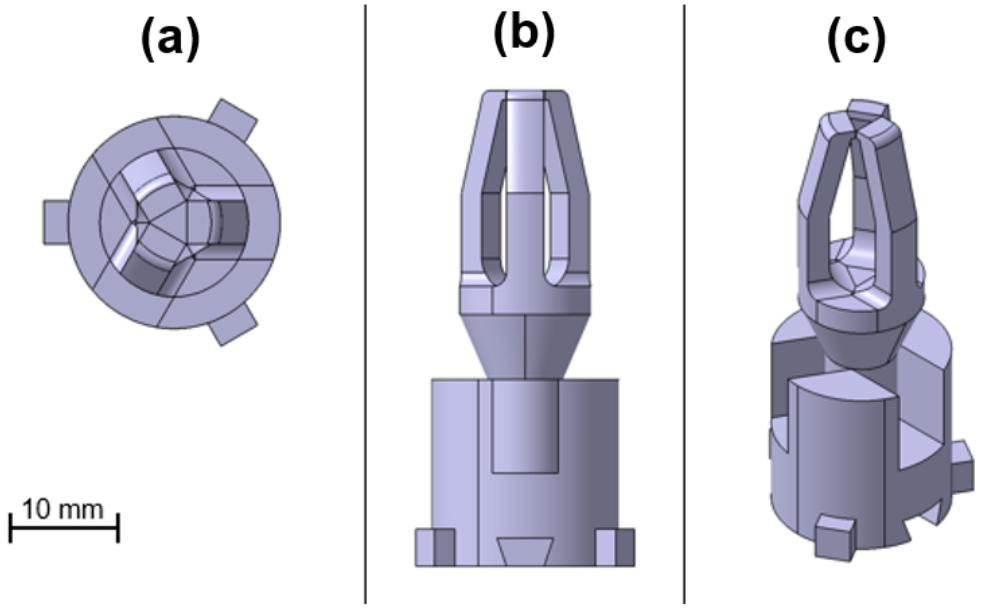

Figure 4. First design of the gripping system in different views: (**a**) top view, (**b**) side view, (**c**) three-dimensional view.

Extraction system:

The extraction system is made of magnetic composite material. A meander structure is used to realize the sub-function. This is initially folded as tightly as possible to not hinder the other subsystems in performing their functions. As soon as the temperature inside the bottle rises above T_G, the PLA matrix of the composite material becomes deformable and enters the thermoelastic state. Here, it can be deformed with low force but retains its magnetic properties due to the iron particles it contains since the Curie temperature of the iron particles is not exceeded. Via the cuboidal plateau at the end of the extraction system, a bar magnet is used to interact with the iron particles contained in the PLA matrix to attract them and eventually unfold the meander structure of the extraction system by moving upwards. In this way, a manually accessible connection of the component to the neck of the bottle is created, through which the target object can be recovered. A rail attached to the underside of the extraction system creates a form-fitting connection with the gripping system. Figure 5 shows the first design of the extraction system in different views.

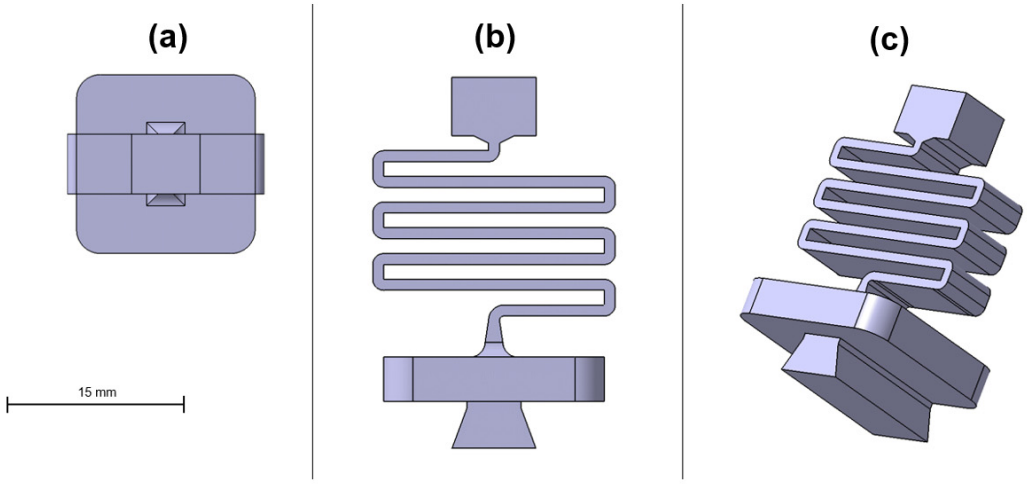

Figure 5. First design of the extraction system in different views: (**a**) top view, (**b**) side view, (**c**) three-dimensional view.

3.3.2. Analysis, Dimensioning, and Optimization of the First Designs

First, the positioning and gripping subsystems made of an SMP are tested for functional performance. Initial tests with prototypes have shown that the degree of shape recovery varies considerably. This suggests that the shape recovery capability (SRC) of SMPs depends on various factors that have to be determined before testing the prototypes of the first designs. Identifying and using the ideal parameters for shape recovery ensures that results can be reproduced reliably and that the maximum potential of the SMP is achieved.

The influential factors for the SRC and their associated optimum values for the shape recovery of the SMP material are determined by the following on the basis of a series of tests. For this purpose, controllable influencing factors are first compiled. These include:

- The heating time t_H;
- The cooling time t_C;
- The duration of the external force application t_{deform};
- The deformation temperature T_{Deform};
- The shape recovery temperature T_{SR}.

During the test series, only one of the influencing factors mentioned is changed, and the effect of this change on the SRC is measured. All other influencing factors remain unchanged. Three identical test objects are used to investigate each influencing factor. For each of the three test objects, the value of the corresponding influencing factor is changed and the result is documented. The test object is a gripper especially developed for this series of tests, whose design is based on the first design of the gripping system. In order to quantify and compare the SRC of the test objects, it is defined as follows:

$$R_{SR} = \frac{\gamma_{SR}}{\gamma_{deformation}} \tag{1}$$

The angles included in the calculation of R_{SR} are the angles after initial deformation $\gamma_{deformation}$ and the angles after shape recovery γ_{SR}. These are schematically illustrated in Figure 6.

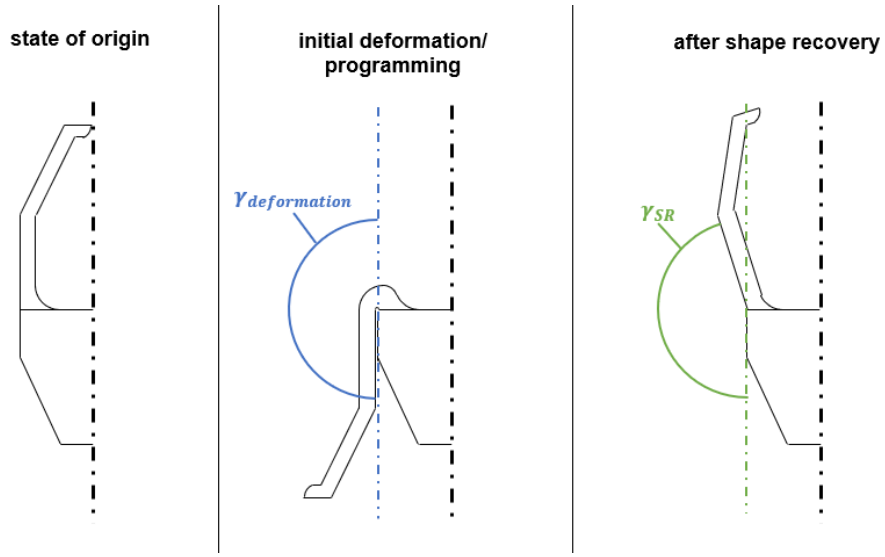

Figure 6. Schematic illustration of the angles $\gamma_{deformation}$ and γ_{SR} included in the calculation of R_{SR}.

In addition to the above-mentioned influencing factors, the test series investigates how the material behaves in terms of shape recovery when $T_{Deform} = T_{SR}$. The standard parameters for the entire test series are chosen as follows:

- Heating time $t_H = 120$ s;
- Cooling time $t_C = 300$ s;
- Duration of the external force application $t_{deform} = 90$ s;
- Deformation temperature $T_{Deform} = 85$ °C;
- Shape recovery temperature $T_{SR} = 85$ °C.

The printing parameters stay the same for every specimen and are shown in Table 3. The printing parameters have been determined by preliminary tests or are predefined by specifications. The decisive factors for the chosen parameters were frugality, duration of printing, and sustainability.

Table 3. Printing parameters for the specimen.

Printing Parameters	Unit	Value
Layer height	mm	0.15
Infill	%	70
Print speed	mm/s	45 (perimeter), 80 (infill)
Nozzle temperature	°C	230
Print bed temperature	°C	60

The results of the test series are shown in Table 4.

Table 4. Results of the test series.

		Test Object 1		Test Object 2		Test Object 3	
Investigated Factor	**Unit**	**Test Value 1**	R_{SR}	**Test Value 2**	R_{SR}	**Test Value 3**	R_{SR}
Heating time t_H	s	60	92.2%	120	91.7%	180	89.4%
Cooling time t_C	s	120	91.7%	300	92.8%	600	90.6%
Duration of external force t_{deform}	s	45	91.1%	90	91.7%	180	91.7%
Deformation temperature T_{deform}	°C	85	91.7%	75	80.6%	65	82.8%
Shape recovery temperature T_{SR}	°C	85	91.1%	75	91.7%	65	88.3%
$T_{deform} = T_{SR}$	°C	85	90.6%	75	94.4%	65	96.7%

It is important to mention that a value of approximately $R_{SR} = 92\%$ is a sufficient result for reliable gripping of an object. The results of the test series show that the decisive influencing factors on the SRC of the material are the deformation temperature T_{deform} and the shape recovery temperature T_{SR}. At $T_{deform} = T_{SR} = 65$ °C, the best overall result of the test series is obtained, and this could not be achieved for any other influencing factor. According to the results, the SRC of the material increases the closer the value approaches the T_G of the material, which lies between 55 °C and 60 °C. For all other influencing factors investigated, it appears that a change in the test values has no remarkable effect on the SRC. Based on the results, the following parameters for optimum shape recovery can be derived for the material used:

- Duration of heating $t_H = 60$ s;
- Duration of cooling $t_C = 300$ s;
- Duration of the external force application $t_{deform} = 90$ s;
- Temperature during deformation $T_{deform} = 65$ °C;
- Temperature during shape recovery $T_{SR} = 65$ °C.

Now, on the basis of these findings, the subsystems produced from an SMP are tested for their functional performance.

Positioning system:

The function of the positioning system is considered to be fulfilled when the component is in a stable position above the center of the bottle base after the shape recovery. For this purpose, it is brought into its temporary shape, taking into account the optimum parameters for shape recovery, and placed in the test environment. Then, the SME is triggered by heating the component above T_G using tempered water. Figure 7 summarizes the test procedure.

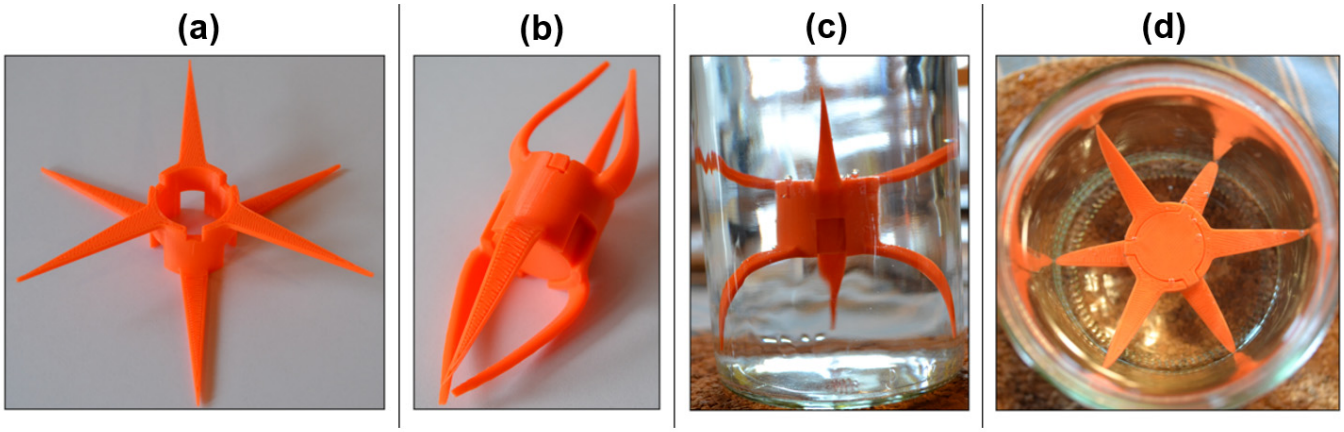

Figure 7. (**a**) Prototype of the positioning system in the initial state, (**b**) temporary form of the positioning system after the programming phase, (**c**) lateral view after the shape recovery of the positioning system, (**d**) view from above after the shape recovery of the positioning system.

After testing the prototype, the results show that the positioning system positions itself over the center of the bottle base as intended after the stimulus is applied. This condition is repeatedly and reliably achieved after several tests. Therefore, the successfully tested concept of the six-arm positioning system is maintained. The next step consists of dimensioning and optimizing the design to properly fit the application example.

First, the positioning system is designed to position itself at a desired height above the center of the bottle base. The length of the arms is decisive for the height at which it is located after the shape recovery. To ensure optimum gripping of the gripper system, the positioning system should be 40 mm above the center of the bottle base after the shape recovery. The six-arm system ensures central alignment. The geometries to be considered for the design are shown in Figure 8. The trigonometric functions are used to calculate the arm length required to achieve the desired height of 40 mm. Since a curvature of the arms takes place during shape recovery, 8 mm is added to the calculated value to compensate adequately. This results in a value of r = 52.7 mm as the arm length. The thickness of the arms is set to 2 mm.

The round, central part of the positioning system with the borehole has an outer diameter of 30 mm to not exceed the permitted width (B_{per}). In addition, the length of the middle part is set to 50 mm. If the length of the middle part was too short, the inclined position of the entire system would push the target object off its base before the shape recovery process begins. In addition, the arms are integrated into the top and bottom ends. This facilitates the deformation of the arms during the programming phase of the SMP, and the curvature of the arms is reduced at the same time. The wall thickness is set to 2.5 mm. The target object is later guided through the interior of the positioning system with a diameter of the remaining 25 mm to be extracted from the bottle using the gripping and extraction system. Figure 9 shows the final design of the positioning system in different views.

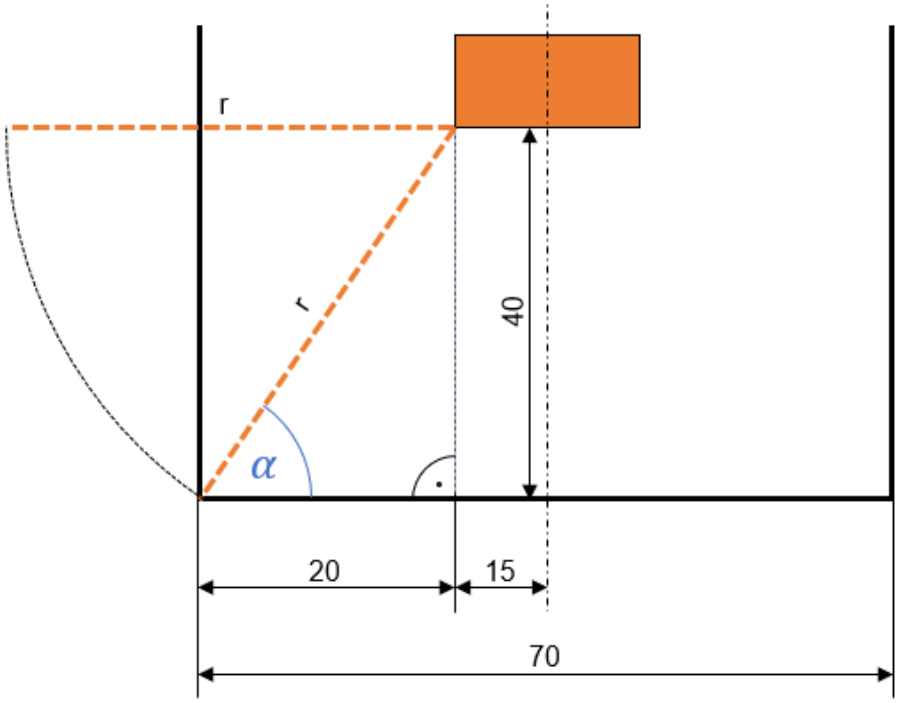

Figure 8. Schematic illustration of the geometry to be considered for the positioning system.

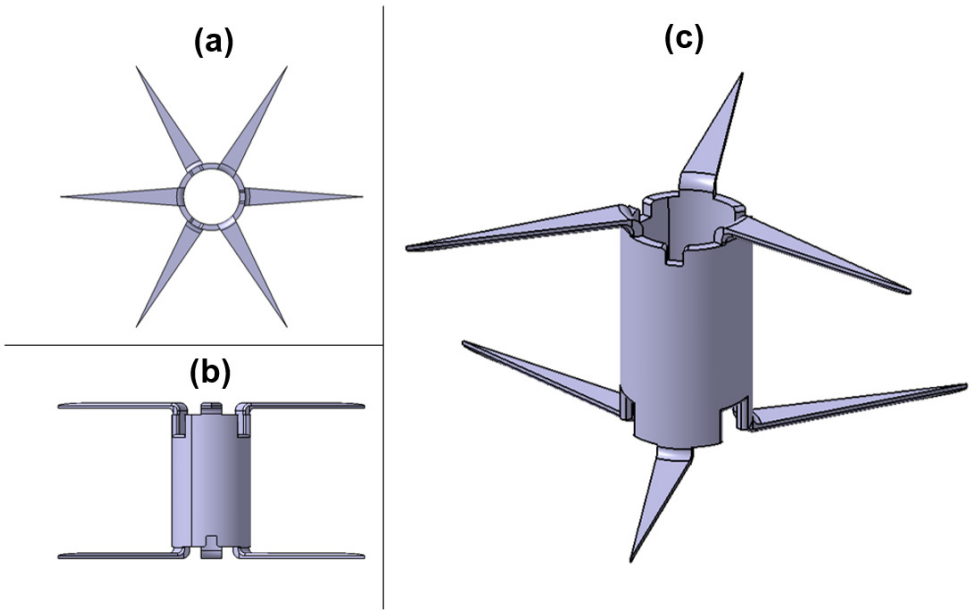

Figure 9. Final design of the positioning system in different views: (**a**) top view, (**b**) side view, (**c**) three-dimensional view.

Gripping system:

To fulfill its function, the gripping system must be able to grip the target object firmly. Again, the determined optimal parameters for the SRC of the material are used. In preparation, the gripper arms of the gripping system are brought into a wide-open shape during the programming phase of the SMP by folding them backward by almost 180° into the inserted pockets. Figure 10 summarizes the test procedure.

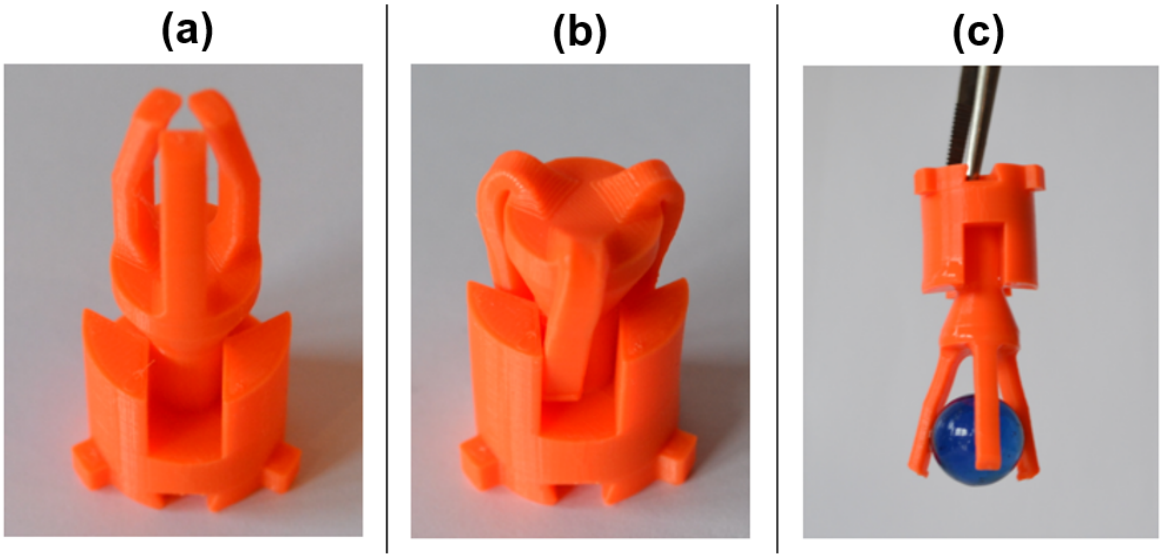

Figure 10. (**a**) Prototype of the gripping system in the initial state, (**b**) temporary shape of the gripping system with wide-open grippers, (**c**) after shape recovery while gripping the target object.

The test shows that the gripping system is capable of gripping the target object and lifting it. The basic concept of the gripping system is, therefore, maintained. To further improve the gripping process and make it more reliable, the gripping system will be dimensioned and optimized for the application example in the next step.

When performing its function, the gripping system is exactly 40 mm centered above the target object due to the previous alignment with the help of the positioning system. The center of the round target object is located on a base at a height of 18 mm above the bottom of the bottle. The gripping system must grip the target object below this height in any case; otherwise, it cannot be gripped firmly. It is essential that this is considered in the design. For this reason, the gripper arms will have a total length of 21.5 mm, while the plateau on which the gripper arms are located will have a length of 15 mm. As a result of that the target object will be gripped below its center point in any case. The diameter of the plateau on which the three gripper arms are located should be kept as small as possible. This ensures that the target object can be gripped even if the shape recovery is not optimal. The diameter is set to 16 mm.

The central body of the gripping system is 50 mm long to match the length of the central part of the positioning system into which the gripping system is later integrated. However, the diameter of the central body is selected to be significantly smaller than the 25 mm inner diameter of the positioning system, as otherwise, the gripping and positioning system tend to tilt due to thermal distortion and slight deformation. This problem is prevented by adjusting the diameter. The diameter is, therefore, set to 22 mm to allow a 1.5 mm tolerance on each side.

The gripper arms of the gripper are 5 mm wide and 3 mm thick. The dimensions have been deliberately chosen to be larger than the dimensions of the arms of the positioning system, which are 2 mm in thickness. Various tests have shown that thicker components require more time to activate the SME. Based on the knowledge gained from this observation, the shape recovery of the gripping arms is deliberately delayed so that it starts after the positioning by the positioning system. The final design is shown in various views in Figure 11.

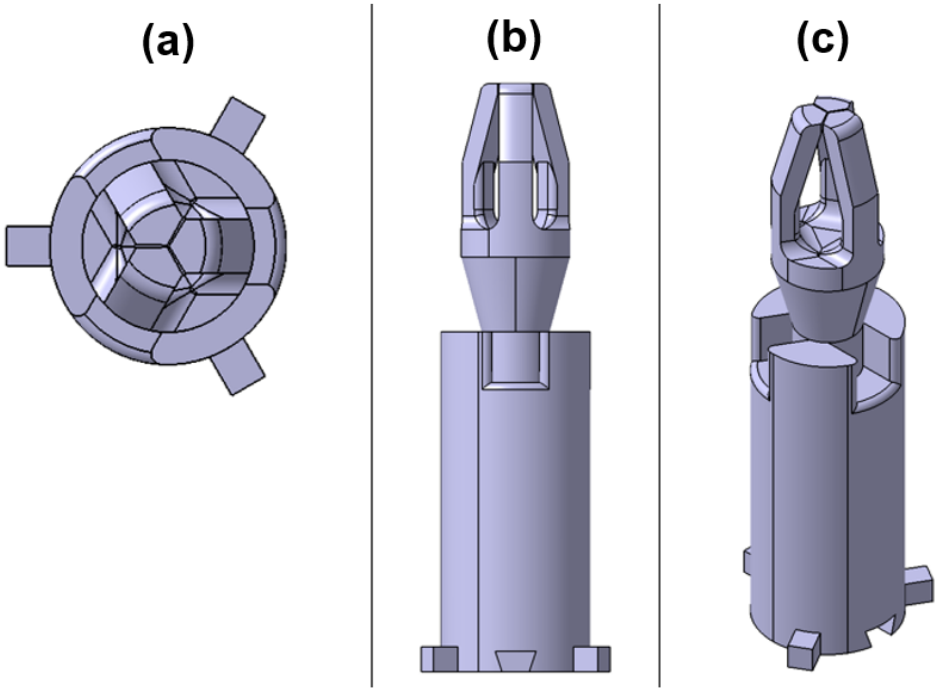

Figure 11. Final design of the gripping system in different views: (**a**) top view, (**b**) side view, (**c**) three-dimensional view.

Extraction system:

In order for the extraction system to fulfill its function, it has to create a manually accessible connection to the bottleneck for recovering the target object. To test the functional performance, the prototype extraction system is heated above its T_G and then deformed. Figure 12 shows the magnetic extraction system in various states during testing.

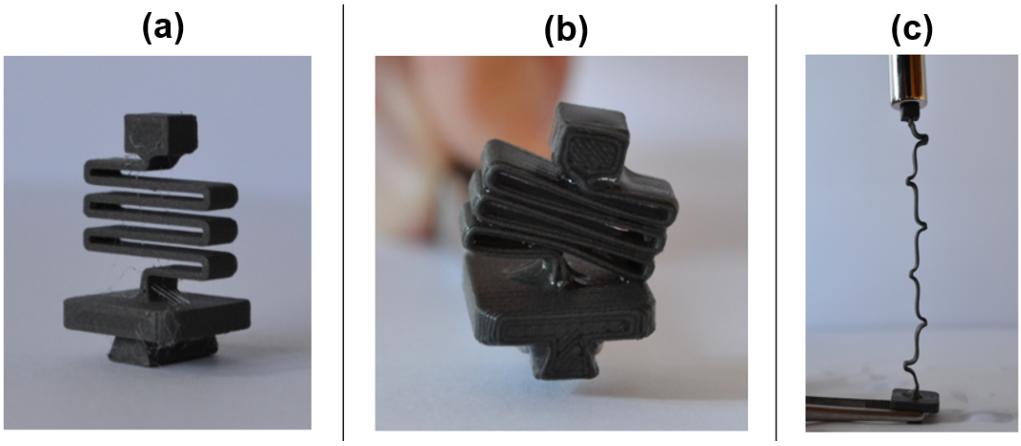

Figure 12. (**a**) Prototype of the extraction system in the initial state, (**b**) extraction system after heating above T_G, (**c**) extraction system after deformation by interacting with a magnet.

The experimental results show that the extraction system in the thermoelastic state can be deformed as intended under the influence of the magnetic field. By unfolding the meander structure, the extraction system is able to successfully fulfill its sub-function. Therefore, for the final design, the basic design of the first design is maintained. The proper dimensioning and optimization will be performed in the next step.

The cuboid, which serves as the foundation for the meander structure, has a side length of 15 mm. At this size, the extraction system fits exactly on the top of the gripping system, to which it is attached via the rail.

To establish a manually accessible connection, a distance of at least 90 mm has to be overcome. This must be taken into account in the calculation of the turns of the meander structure. A cross strut is 17 mm long and 0.75 mm wide. Accordingly, at least five cross struts are required. However, since this is not sufficient due to the non-linear final shape, as can be seen in Figure 12c, seven cross struts are used. In addition, an uneven number of cross struts ensures an ideal weight distribution and thus prevents the structure from tilting sideways while it is deformable. To further prevent the structure from tilting, two cuboids are positioned under the cross struts to act as a support platform. In addition, the depth of the meander structure is increased to 9 mm to prevent it from tilting backward or forward.

Finally, the plateau at the upper end of the meander structure, to which the magnetic field is applied, is enlarged. This enlargement allows more of the iron particles in the composite to be attracted by the magnetic field, making the interaction with the magnet much easier. The final design of the extraction system can be seen in various views in Figure 13.

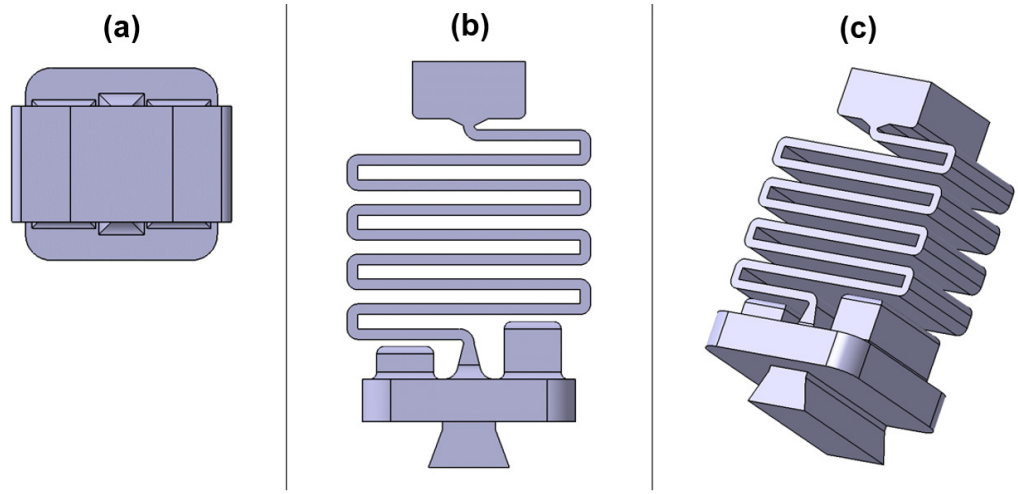

Figure 13. Final design of the extraction system in different views: (**a**) top view, (**b**) side view, (**c**) three-dimensional view.

Overall system:

For illustration purposes and to present the final design of the overall system, Figure 14 shows the overall system in the form of an assembly consisting of the different subsystems.

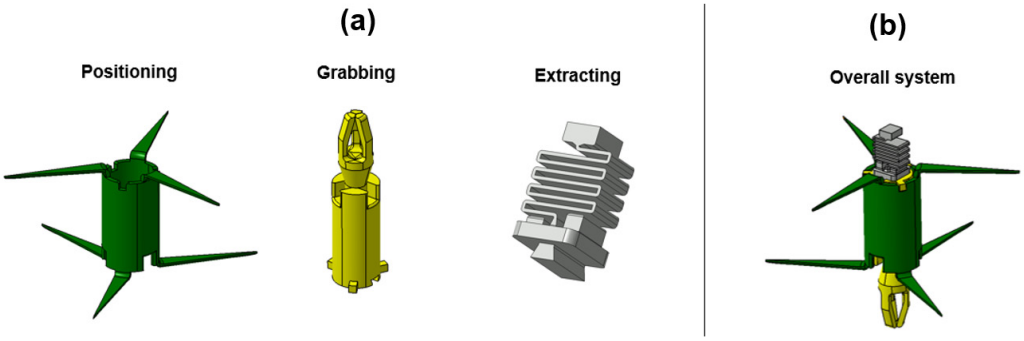

Figure 14. (**a**) Final designs and CAD models of the subsystems, (**b**) final design and virtually assembled CAD model of the complete system based on [31].

3.4. Manufacturing

The STL files of the CAD models of the subsystems are used as the input for the additive manufacturing process. All subsystems are manufactured with a Prusa i3 MK3S+. This 3D printer works according to the MEX process, in which a thermoplastic is melted

by using a heated nozzle and extruded onto the build platform in order to build up the component layer by layer. A 0.4 mm diameter nozzle was used to print the specimen. All printing parameters are the same as in Table 3. Once the components have been successfully printed, they are programmed and assembled into the overall system to make it ready for use. To perform this, the first step is to put the gripping system into its temporary form. The extraction system is then connected to the gripping system via the rail. Subsequently, the positioning system is heated above T_G and the assembled subsystems are integrated into the pockets of the positioning system. Now the six arms of the positioning system, which are still deformable, are folded evenly up and down so that they converge at the extended axis of the center bore of the center cylinder. Once these steps are completed, the component is ready for deployment. The assembling and programming are summarized in Figure 15.

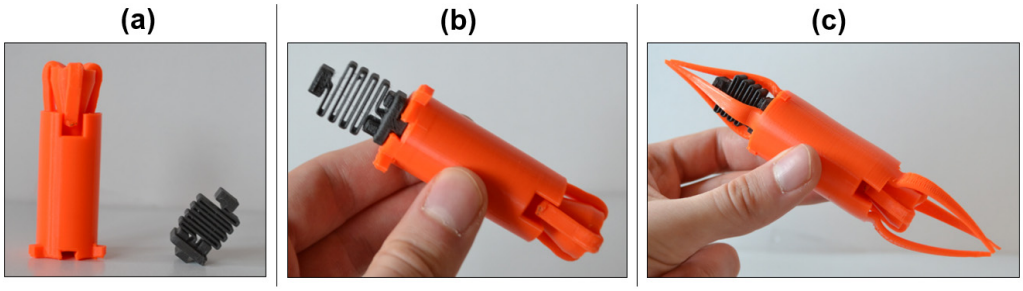

Figure 15. (**a**) Programmed positioning system with extraction system, (**b**) connection of the two subsystems via the rail, (**c**) integration of the two subsystems into the positioning system and programming.

3.5. Application of the Component

The first step is to place the component in the bottle. By filling the bottle with tempered water at a temperature of 65 °C, the SME of the positioning and gripping system engages. As a result, the component first positions itself over the target object using the six arms, before engaging with the three gripper arms. As planned, the snake-shaped structure of the extraction system becomes deformable. It can be easily unfolded by interacting with a magnet.

By pulling the extraction system upwards, the target is removed from the bottle. The positioning system remains in the bottle. It can be observed that all subsystems fulfill their function reliably, whereby the given task of recovering the target object is solved successfully. Figure 16 shows the use of the overall system at various times during the recovery operation. The whole process can be seen in Video S1 in the Supplementary Materials.

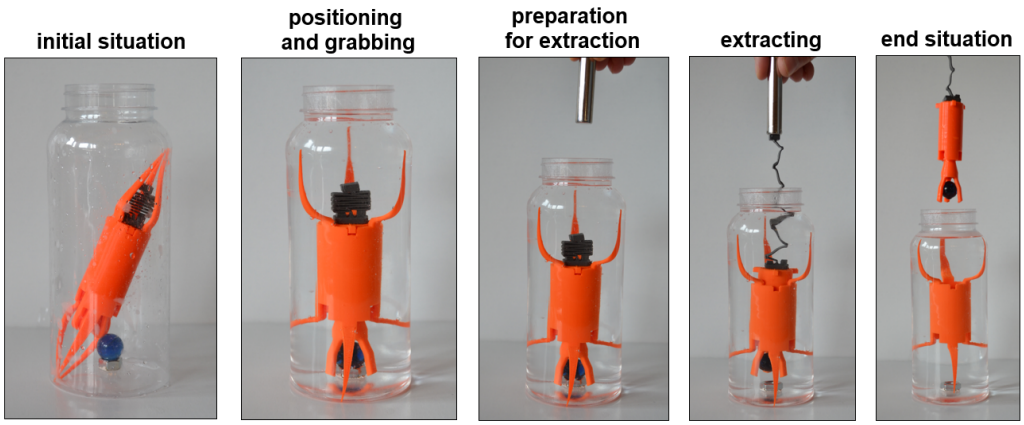

Figure 16. Use of the overall system at different points in time [31].

4. Conclusions

The results show that the presented methodical approach for the development of 4D-printed components can be successfully used to solve a given problem. However, the

application example clearly shows the limitations of complexity based on the early stage of development of 4D printing technology. In order for 4D printing technology to establish itself alongside other technologies in the future, it is also necessary to be able to solve more complex problems. The method presented here offers a methodical approach that can also be applied to more complex tasks since the focus is on a holistic and problem-solving approach. In addition, the methodical approach is a novelty and offers an initial approach as to how the current findings from research in the field of 4D printing can be transferred to application in a structured and useful way. This is crucial for the further development of 4D printing technology and for making it a competitive alternative to existing technologies.

By analyzing and using the SMP and the magnetic composite material, the potentials of the two smart materials are investigated in more detail. The most significant disadvantage of the SMPs is their limited reversibility. Here, the magnetic composite materials promise a great amount of potential in terms of reversibility, reaction time, and controllability of the stimulus. For the realization of complex movements, certain magnetic properties of the contained magnetic particles, such as sufficient remanence and coercivity, are crucial. However, since a PLA matrix with embedded iron particles is used in this work, the potentials mentioned cannot be fully exploited. The development of these potentials is setting a trend for the technology of 4D printing, which is already impressively shown in the literature. Further research projects of the authors will, therefore, focus on the use of magnetic composite materials with suitable and tailored magnetic properties in order to realize complex changes in the shape or function of the components and thus tie in with the existing research.

Supplementary Materials: The following supporting information can be downloaded at: https://www.mdpi.com/article/10.3390/machines11111035/s1, Video S1: Video of 4D printing.

Author Contributions: Conceptualization, S.J., H.E. and D.V.; methodology, S.J., H.E. and D.V.; software, H.E.; validation, S.J., H.E. and D.V.; formal analysis, S.J., H.E. and D.V.; investigation, S.J., H.E. and D.V.; resources, S.J., H.E. and D.V.; data curation, H.E.; writing—original draft preparation, S.J., H.E. and D.V.; writing—review and editing, S.J., H.E. and D.V.; visualization, S.J., H.E. and D.V.; supervision, S.J. and D.V.; project administration, S.J. and D.V.; funding acquisition, none. All authors have read and agreed to the published version of the manuscript.

Funding: We acknowledge support by the Open Access Publication Fund of the Offenburg University of Applied Sciences.

Data Availability Statement: Data are contained within the article or Supplementary Materials.

Conflicts of Interest: The authors declare no conflict of interest.

References

1. Tibbits, S. 4D Printing: Multi-Material shape change. *Archit. Des.* **2014**, *84*, 116–121. [CrossRef]
2. Quanjin, M.; Rejab, M.R.M.; Idris, M.S.; Kumar, N.M.; Abdullah, M.H.; Reddy, G.R. Recent 3D and 4D intelligent printing technologies: A comparative review and future perspective. *Procedia Comput. Sci.* **2020**, *167*, 1210–1219. [CrossRef]
3. Zafar, M.Q.; Zhao, H. 4D Printing: Future Insight in Additive Manufacturing. *Met. Mater. Int.* **2020**, *26*, 564–585. [CrossRef]
4. Zhang, J.; Yin, Z.; Ren, L.; Liu, Q.; Ren, L.; Yang, X.; Zhou, X. Advances in 4D Printed Shape Memory Polymers: From 3D Printing, Smart Excitation, and Response to Applications. *Adv. Mater. Technol.* **2022**, *7*, 2101568. [CrossRef]
5. Kantaros, A.; Ganetsos, T.; Piromalis, D. 4D Printing: Technology Overview and Smart Materials Utilized. *J. Mechatron. Robot.* **2023**, *7*, 1–14. [CrossRef]
6. Momeni, F.; Hassani, S.M.M.; Liu, X.; Ni, J. A review of 4D printing. *Mater. Des.* **2017**, *122*, 42–79. [CrossRef]
7. Pei, E.; Loh, G.H.; Nam, S. Concepts and Terminologies in 4D Printing. *Appl. Sci.* **2020**, *10*, 4443. [CrossRef]
8. Ponnamma, D.; Reddy, M.S.B.; Maurya, M.R.; Kulkarni, O.; Paswan, M.; Sadasivuni, K.K.; Geetha, M.M.M.N.; Al-Maadeed, M.A. Recent Developments on 4D Printings and Applications. In *Shape Memory Composites Based on Polymers and Metals for 4D Printing*; Maurya, M.R., Sadasivuni, K.K., Cabibihan, J., Ahmad, S., Kazim, S., Eds.; Springer: Cham, Switzerland, 2022; pp. 361–388.
9. Imrie, P.; Jin, J. Polymer 4D printing: Advanced shape-change and beyond. *J. Polym. Sci.* **2021**, *2*, 149–174. [CrossRef]
10. Chu, H.; Yang, W.; Sun, L.; Cai, S.; Yang, R.; Liang, W.; Yu, H.; Liu, L. 4D Printing: A Review on Recent Progresses. *Micromachines* **2020**, *11*, 796. [CrossRef]
11. Champeau, M.; Heinze, D.A.; Viana, T.N.; de Souza, E.R.; Chinellato, A.C.; Titotto, S. 4D Printing of Hydrogels: A Review. *Adv. Funct. Mater.* **2020**, *30*, 1910606. [CrossRef]

12. Khosravani, M.R.; Soltani, P.; Weinberg, K.; Reinicke, T. Structural integrity of adhesively bonded 3D-printed joints. *Polym. Test.* **2021**, *100*, 107262. [CrossRef]
13. Sharma, A.; Mukhopadhyay, T.; Kushvaha, V. Experimental data-driven uncertainty quantification for the dynamic fracture toughness of particulate polymer composites. *Eng. Fract. Mech.* **2022**, *273*, 108724. [CrossRef]
14. Ge, Q.; Sakhaei, H.; Lee, H.; Dunn, C.K.; Fang, N.X.; Dunn, M.L. Multimaterial 4D Printing with Tailorable Shape Memory Polymers. *Sci. Rep.* **2016**, *6*, 31110. [CrossRef]
15. Wei, H.; Zhang, Q.; Yao, Y.; Liu, L.; Liu, Y.; Leng, J. Direct-Write Fabrication of 4D Active Shape-Changing Structures Based on a Shape Memory Polymer and Its Nanocomposite. *ACS Appl. Mater. Interfaces* **2017**, *9*, 876–883. [CrossRef]
16. Alshebly, Y.; Nafea, M. Control of 4D Printed Actuators Twisting Behavior via Printing Direction. In Proceedings of the 2022 IEEE 20th Student Conference on Research and Development (SCOReD), Bangi, Malaysia, 8–9 November 2022; IEEE: Piscataway, NJ, USA, 2022; pp. 163–167.
17. Zhou, Y.; Huang, Z.; Li, X.; Lv, P. 4D Printing Pre-Strained Structures for Fast Thermal Actuation. *Front. Mater.* **2021**, *8*, 661999. [CrossRef]
18. Nezhad, I.; Golzar, M.; Behravesh, A.; Zare, S. Comprehensive study on shape shifting behaviors in FDM-based 4D printing of bilayer structures. *Int. J. Adv. Manuf. Technol.* **2022**, *120*, 959–974. [CrossRef]
19. Zhang, J.; Ji, D.; Yang, X.; Zhou, X.; Yin, Z. 4D printing of bilayer structures with programmable shape-shifting behavior. *J. Mater. Sci.* **2022**, *57*, 21309–21323. [CrossRef]
20. Kuang, X.; Roach, D.; Wu, J.; Hamel, C.; Ding, Z.; Wang, T.; Dunn, M.; Qi, H. Advances in 4D Printing: Materials and Applications. *Adv. Funct. Mater.* **2019**, *29*, 1805290. [CrossRef]
21. Raviv, D.; Zhao, W.; McKnelly, C.; Papadopoulou, A.; Kadambi, A.; Shi, B.; Hirsch, S.; Dikovsky, D.; Zyracki, M.; Olguin, C.; et al. Active Printed Materials for Complex Self-Evolving Deformations. *Sci. Rep.* **2014**, *4*, 7422. [CrossRef] [PubMed]
22. Baker, A.; Bates, S.; Llewellyn-Jones, T.; Valori, L.; Dicker, M.; Trask, R. 4D printing with robust thermoplastic polyurethane hydrogel-elastomer trilayers. *Mater. Des.* **2019**, *163*, 107544. [CrossRef]
23. Bakarich, S.E.; Gorkin, R.; in het Panhuis, M.; Spinks, G.M. 4D Printing with Mechanically Robust, Thermally Actuating Hydrogels. *Macromol. Rapid Commun.* **2015**, *36*, 1211–1217. [CrossRef] [PubMed]
24. Zu, S.; Zhang, Z.; Liu, Q.; Wang, Z.; Song, Z.; Guo, Y.; Xin, Y.; Zhang, S. 4D printing of core–shell hydrogel capsules for smart controlled drug release. *Bio-Des. Manuf.* **2022**, *5*, 294–304. [CrossRef]
25. Abdullah, T.; Okay, O. 4D Printing of Body Temperature-Responsive Hydrogels Based on Poly(acrylic acid) with Shape-Memory and Self-Healing Abilities. *ACS Appl. Bio Mater.* **2023**, *6*, 703–711. [CrossRef]
26. Shiblee, M.N.I.; Ahmed, K.; Kawakami, M.; Furukawa, H. 4D Printing of Shape-Memory Hydrogels for Soft-Robotic Functions. *Adv. Mater. Technol.* **2019**, *4*, 1900071. [CrossRef]
27. Cecchini, L.; Mariani, S.; Ronzan, M.; Mondini, A.; Pugno, N.; Mazzolai, B. 4D Printing of Humidity-Driven Seed Inspired Soft Robots. *Adv. Sci.* **2023**, *10*, 2205146. [CrossRef]
28. Kotikian, A.; Truby, R.; Boley, J.; White, T.; Lewis, J. 3D Printing of Liquid Crystal Elastomeric Actuators with Spatially Programed Nematic Order. *Adv. Mater.* **2018**, *30*, 1706164. [CrossRef]
29. Kim, Y.; Yuk, H.; Zhao, R.; Chester, S.A.; Zhao, X. Printing ferromagnetic domains for untethered fast-transforming soft materials. *Nature* **2018**, *558*, 274–279. [CrossRef]
30. Zhang, Y.; Wang, Q.; Yi, S.; Lin, Z.; Wang, C.; Chen, Z.; Jiang, L. 4D Printing of Magnetoactive Soft Materials for On-Demand Magnetic Actuation Transformation. *ACS Appl. Mater. Interfaces* **2021**, *13*, 4174–4184. [CrossRef] [PubMed]
31. Junk, S.; Einloth, H.; Velten, D. A Methodical Approach to Product Development in 4D Printing Using Smart Materials. In *Progress in Digital and Physical Manufacturing*; Proceedings of ProDPM'21; Almeida, A.H., Vasco, J.C., Eds.; Springer: Cham, Switzerland, 2023; pp. 130–137.
32. VDI—The Association of German Engineers, VDI 2221. Systematic Approach to the Development and Design of Technical Systems and Products. Available online: https://www.vdi.de/richtlinien/details/vdi-2221-methodik-zum-entwickeln-und-konstruieren-technischer-systeme-und-produkte (accessed on 22 October 2020).
33. Pahl, G.; Beitz, W.; Feldhusen, J.; Grote, K.H. *Engineering Design: A Systematic Approach*; Springer: London, UK, 2007.